

Tailoring of pre-existing flaws in ECC matrix for saturated strain hardening

Shuxin Wang & Victor C. Li

Advanced Civil Engineering Materials Research Laboratory

Department of Civil and Environmental Engineering

The University of Michigan, Ann Arbor, Michigan, U.S.A.

ABSTRACT: Strain-hardening and magnitude of ductility in high performance fiber reinforced composites are closely related to matrix properties, e.g. the pre-existing flaw size distribution and the matrix fracture toughness. For a brittle matrix composite such as ECC, cracking strength is determined by the largest flaw in the section normal to the maximum principle stress. The maximum fiber bridging stress imposes a lower bound of critical flaw size such that only those flaws larger than this critical size can be activated and contribute to multiple cracking. Insufficient number of large flaws in the matrix causes unsaturated multiple cracking. A practical approach to controlling the pre-existing flaws, i.e. introducing artificial flaws with prescribed size distribution, is proposed in this paper. This approach was verified in two versions of PVA-ECC where multiple cracking is hindered by high matrix toughness. Direct uniaxial tension test results confirmed the validity of the proposed material tailoring approach.

Keywords: strain hardening, multiple cracking, flaw size distribution, engineered cementitious composite

1 INTRODUCTION

In the past decade, great stride has been made in developing high performance fiber-reinforced cementitious composites (HPFRCC) characterized by multiple-cracking and strain-hardening behavior under uniaxial tension (Naaman & Reinhart 1996). This advance is mainly due to the better understanding of the micromechanics governing composite behavior, i.e. the interaction between fiber, matrix and interface properties. In particular, most efforts focused on the fiber bridging properties and result in the establishment of various micromechanics models based on different approaches (e.g. Li 1992, Lin et al. 1999, Naaman & Reinhart, 1996). These models later led to successful engineering of fiber and interface properties for creating high ductility composites with low fiber volume fraction, for instance, Engineered Cementitious Composites (ECC) by tailoring fiber geometry interface properties and matrix toughness (Li et al. 2002), and Torex-HPFRC by engineering the shape, size, and mechanical properties of steel fiber (Sujivorakul 2002).

As multiple cracking behavior is generally observed in these HPFRCC materials, the density of cracks or the cracking spacing varies significantly from material to material, even within different versions of the same class of material. Since the inelastic tensile strain of HPFRCC derives from development of multiple cracking, large crack spacing means that the potential of reinforcing fibers is not effectively utilized. Assuming that the matrix cracking strength is uniform at each section, Aveston et al. (1971) and later Wu & Li (1992) derived minimum cracking spacing x_d for aligned continuous fiber and random short fiber reinforced composites respectively. Under this assumption, a final crack spacing between x_d and $2x_d$ is expected after crack saturation. However, in HPFRCC uniaxial tension specimens a wide distribution far exceeding two times of minimum cracking spacing is often observed, due to the variation of both matrix properties and fiber distribution.

For a brittle matrix composite such as HPFRCC, cracking strength is determined by the matrix fracture toughness and the largest crack-like flaw in the section normal to the maximum principle stress, provided that the matrix cracking is

controlled by a fracture process. The significance of controlling matrix fracture toughness in ECC mix design to achieve strain-hardening has been demonstrated by Li et al. (1995), where low matrix toughness leads to high strain capacity for given fiber and interface properties. As various inherent flaws exist in cementitious matrix, e.g. pores, weak boundary between phases, and cracks induced by shrinkage, the size and spatial distribution of these pre-existing flaws possess random nature and strongly depend on processing details and environmental effects. Wu & Li (1995) investigated the effect of matrix flaw size distribution on composite strength and cracking spacing by a Monte Carlo process, where the flaw size distribution is assumed to follow Weibull distribution, and good agreement between the experiment data and simulation results is found for a polyethylene fiber reinforced cement paste.

The objective of this paper is to investigate the viability of achieving saturated multiple cracking by controlling the pre-existing flaw size distribution in ECC, a special family of HPFRCC featuring high strain capacity in tension and moderate fiber volume fraction (typically below 2.5%). Saturated multiple cracking has been demonstrated in several ECC versions, where the fiber, interface and matrix properties are carefully tailored under the guidance of micromechanical principles (Li 1998, Li et al. 2002). In general, matrix with low matrix toughness is adopted in the mix design of these ECC materials in order to promote multiple cracking, leaving the flaw size distribution solely determined by the mix proportion and processing details. In some applications, however, low matrix fracture toughness may not be easily achievable while other functional requirements such as early age strength, elastic modulus and workability impose constraints on the composition and proportion of matrix mix design. Although the criteria of strain hardening, which will be discussed in detail in Section 2, may be still satisfied in these cases, the number of cracking and in turn the strain capacity often deteriorate considerably due to the tougher matrix. Meanwhile, variation in ductility performance is also observed when the processing details change. For example, cracking behavior can be significantly different for the same mix prepared by extrusion process and by normal casting process, where the flaw size distribution is altered by the processing details. In order to achieve a robust mechanical performance, therefore, a build-in mechanism of flaw size control is preferred in mix design.

A practical approach to controlling the pre-existing flaws, i.e. introducing artificial flaws with prescribed size distribution, is proposed in this paper. Since it is difficult to quantitatively characterizing the natural flaw system and further to control the size distribution in various processing conditions, the approach proposed here is to superpose a prescribed flaw system to the pre-existing flaws. It may not be optimal, but is a feasible and reliable way to ensure sufficient number of large flaws in the matrix. Rigid particles with low strength or weak bond to cementitious matrix are preferred as artificial flaws due to its capability to retain size during processing. In this feasibility study, small lightweight aggregate and plastic beads are selected for this purpose. In the following, the micromechanics criteria for saturated multiple cracking will be first reviewed. The experimental investigation on the effect of artificial flaws in two PVA fiber reinforced ECC materials will then be reported and followed by the discussion where the effectiveness of the proposed matrix tailoring approach is highlighted.

2 MICROMECHANICS THEORETICAL GUIDELINE

In order to achieve strain hardening, steady state cracking must prevail, i.e., the crack length increase at constant ambient stress σ_{ss} while the part of crack profile except crack tip remains flat with a constant crack opening δ_{ss} (Aveston et al. 1971, Li & Leung, 1992; Leung 1996). When the fiber bridging behavior is characterized as bridging stress vs. crack opening relationship ($\sigma(\delta)$ curve, as shown in Fig. 1), the condition of steady state cracking can be expressed as Equation 1, where J_{tip} approaches the matrix toughness K_m^2/E_m at low fiber content. Since the maximum steady state cracking stress cannot exceed the peak fiber bridging stress σ_0 , an upper limit of the matrix fracture toughness can be obtained (Equ. 2), where J_b' is the complementary energy of the $\sigma(\delta)$ curve.

Equation 2, which indeed is based on energy balance, is a necessary condition for multiple cracking; however, it does not indicate when the cracking will occur. Assuming that steady state cracking is initiated by the critical flaw on the section oriented normal to the maximum principle stress, sufficiently large flaws need to exist such that the matrix cracking strength σ_c will be lower than the peak bridging stress σ_0 (Equation 3). As shown by Marshall et al. (1985) and Marshall & Cox (1987), σ_c does not decrease indefinitely with

flow size but reaches a lower bound at steady state cracking stress σ_{ss} .

$$J_{tip} = \sigma_{ss} \delta_{ss} - \int_0^{\delta_{ss}} \sigma(\delta) d\delta \quad (1)$$

$$\frac{K_m^2}{E_m} \leq \sigma_o \delta_o - \int_0^{\delta_o} \sigma(\delta) d\delta \equiv J_b' \quad (2)$$

$$\sigma_c \leq \sigma_o \quad (3)$$

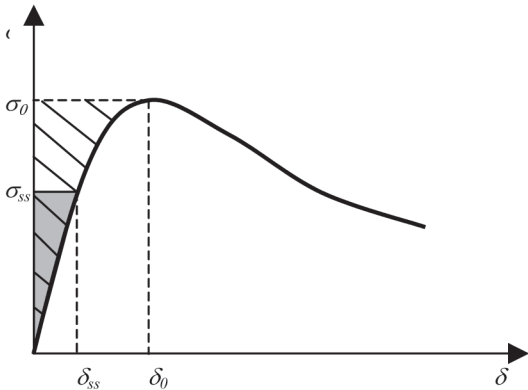


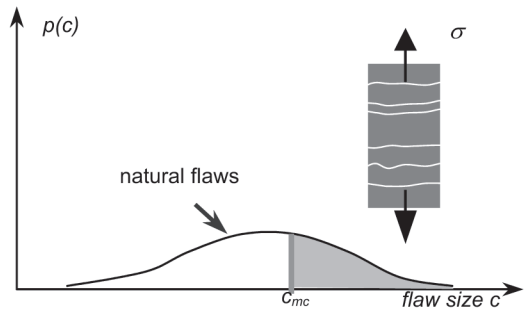
Figure 1. Typical $\sigma(\delta)$ curve for strain hardening material. Shaded area represents right-hand side of Equation 1; Hatched area represents maximum Complementary Energy J_b' of composite.

As Equation 2 and 3 guarantee the occurrence of multiple cracking, the number of the cracks that could be developed is determined by the flaw size and their spatial distribution. Limited by the peak bridging stress, a lower bound of critical flaw size c_{mc} is set such that only those flaws larger than c_{mc} can be activated prior to reaching σ_0 and contribute to multiple cracking. Therefore, to achieve saturated multiple cracking, sufficient number of large flaws must exist in the matrix. c_{mc} here should be regarded as the size of the equivalent Griffith crack that has the same critical stress σ_0 for propagation as the real crack, and apparently it is also determined by matrix toughness. In normal ECC mix without explicit control of flaw size distribution, low toughness matrix is often used such that the reduced c_{mc} would produce adequate margin to activate large number of cracks. Kanda & Li (1998) proposed to use the ratio J_b'/J_{tip} as an indicator for this margin, and an empirical criterion $J_b'/J_{tip} > 3$ is suggested based on experimental observation on polyethylene ECC composite.

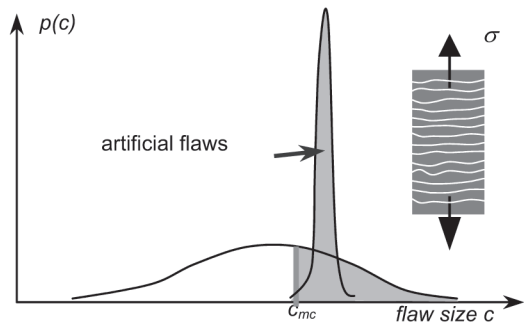
Figure 2 illustrates the concept of the matrix flaw size distribution tailoring scheme for saturated multiple cracking. The introduced artificial flaws have sizes larger than c_{mc} and will be superposed to

the natural flaw system. Since the cracking strength is bounded by steady state stress, larger flaw will not significantly influence the cracking strength. Nevertheless, a narrow size distribution is preferred for the artificial flaws. A lower bound of the content of the artificial flaws can be estimated from the minimum cracking spacing constrained by fiber interface properties and matrix cracking stress, while the upper bound is limited by processing and disturbance of the presence of the relatively large particles on fiber distribution. A complete theoretical model to estimate the optimal size and content of the artificial flaws will be published elsewhere.

The value c_{mc} is critical to prescribe the artificial flaw sizes. In the following experimental program, without indulged in pursuing the accuracy of the theoretical model the size of the particle used as the artificial flaws was selected to be same as the size of the largest voids observed in the cracked sections.



(a) Size distribution of natural flaws in ECC matrix



(b) Size distribution of the superimposed artificial flaws
Figure 2. Scheme of the flaw size tailoring for ECC mix

3 EXPERIMENTAL PROGRAM

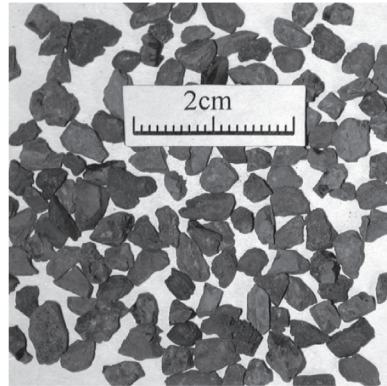
The current investigation is focused on poly vinyl alcohol (PVA) fiber reinforced ECC system, a material gaining increasingly attention in structural application. In order to investigate the influence of the additional artificial flaws on the cracking behaviour, two mixes exhibiting unsaturated multiple cracking were purposely selected as the control mixes. Compared to the PVA-ECC mix proportion in Li et al. (2002) that demonstrated saturated multiple cracking, the mixes used in this study have relatively high matrix toughness due to low water to binder ratio.

Three different particles were used as artificial flaws, including two types of lightweight aggregates and one type of plastic beads. The lightweight aggregates, under the commercial name Norlite, are made from expanded shale and have low tensile strength due to porous microstructure. Two sizes of Norlite particles were tested in this study, with average size 1.0 mm and 3.5 mm respectively. The plastic beads used here are made from polypropylene (PP) and has an elliptical shape and a smooth surface. The length of the long and short axes of the bead is about 4 mm and 2 mm respectively. Since PP has very weak bond to cementitious matrix, the interface will behave like an embedded crack. All three particles are graded and have narrow size distribution. The pictures of the particles are shown in Figure 3.

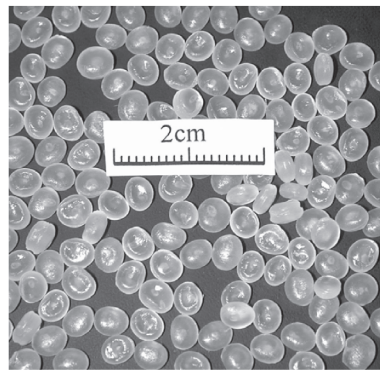
The mix proportions of five mixes, divided into two groups, are listed in Table 1, where mixes in each group share same mix proportion except for the presence of artificial flaws (AF). In Mix5, the small Norlite particles are used to substitute part of the sand. PVA REC15 fiber from Kuraray Co. is used in this study at a fixed volume fraction of 2%. The fiber has a length of 12 mm and a diameter of 39 μm . Details of the fiber properties can be found in Li et al. (2002). Other ingredients include Type I OPC, fine silica sand (average size 110 μm), class C fly ash and superplasticizer (SP).

The mixture was prepared by conventional fiber reinforced concrete preparation procedure. Coupon specimen measuring 304.8 mm x 76.2 mm x 12.7 mm for tension test were cast and cured in water for 28 days before test. The tensile behaviors of the composites were characterized by direct uniaxial tension test under displacement control (details see Li et al. 2002). The loading rate was 0.15 mm/min throughout the test. Two external LVDTs (Linear Variable Displacement Transducer) were attached

to specimen surface with a gage length of about 180 mm to measure the displacement. Average crack spacing was measured after unloading. For the control mixes (Mix 1 and 3), the coupon specimens were sliced normal to the longitudinal direction at the cracked and uncracked sections using a diamond saw, and the cutting surface was observed under optical microscope to examine the large pore size distribution at the section.



(a) Lightweight aggregates used in Mix 2



(b) Polypropylene beads used in Mix 4

Figure 3. Particles used as the artificial flaws

Table 1. Mix proportions

Mix No	Group 1		Group 2		
	Mix 1	Mix 2	Mix 3	Mix 4	Mix 5
Cement	1.0	1.0	1.0	1.0	1.0
Sand	0.8	0.8	0.8	0.8	0.7
FA	0.8	0.8	1.2	1.2	1.2
Water	0.43	0.43	0.53	0.53	0.53
SP	0.03	0.03	0.03	0.03	0.03
Fiber (vol %)	2.0	2.0	2.0	2.0	2.0
AF type	-	Norlite	-	PP	Norlite
AF size (mm)	-	3.5	-	4.0	1.0
AF (vol %)	0	0.07	0	0.07	0.10

All proportions are by weight except fiber and AF.

4 RESULTS AND DISCUSSION

The stress-strain curves of all five mixes are presented in Figure 4-8, and the results in terms of first cracking strength σ_{fc} , ultimate strength σ_{cu} , ultimate strain ϵ_{cu} (e.g. strain at ultimate strength), and crack spacing x_d are summarized in Table 2. The crack pattern of Mix 1-4 is presented in Figure 9-10.

The control mixes exhibit relatively low ductility compared to previously developed PVA-ECC materials (e.g. Li et al. 2003), which strain capacity typically ranges from 3-5%. Micromechanics model reveals that the ratio J_b/J_{tip} , which indicates the potential of developing multiple cracking, is 0.44-1.02 and 0.62-1.24 for Mix 1 and Mix 3 respectively (Wang & Li, in prep.). As mentioned in Section 2, $J_b/J_{tip} > 1$ is a necessary condition for achieving strain-hardening. Mix 1 barely satisfies this condition, and as a result few cracks were developed prior to failure. For Mix 3, the higher J_b/J_{tip} ratio unsurprisingly leads to higher strain capacity. In contrast, the J_b/J_{tip} ratio of the PVA-ECC reported in Li et al. (2002) falls in the range of 4.84-7.62, which is considerably higher than that of the control mixes in this study. Therefore, the margin to develop multiple cracking in Mix 1 and Mix 3 is slim.

The photos of the specimen surface clearly reveal the unsaturated crack patterns of Mix 1 and Mix 3, as displayed in Figure 9a and Figure 10a. Large variation in crack spacing is observed, spanning from 2 mm to 50 mm. Closely spaced cracks can be found locally on both mixes, while there leaves no crack in large areas. It indicates that insufficient number of large flaws existed in the matrix that could be activated, e.g. for such a natural system the shaded area on the flaw size distribution curve (Fig. 2a) is very small.

Table2. Uniaxial tension test results

Mix No	Group 1		Group 2		
	Mix 1	Mix 2	Mix 3	Mix 4	Mix 5
σ_{fc} (MPa)	4.88	4.75	4.06	3.74	3.80
σ_{cu} (MPa)	6.40	6.82	4.84	4.63	4.90
ϵ_{cu} (MPa)	0.38	2.48	1.86	3.79	1.89
x_d (mm)	16.2	2.4	4.8	2.2	4.9

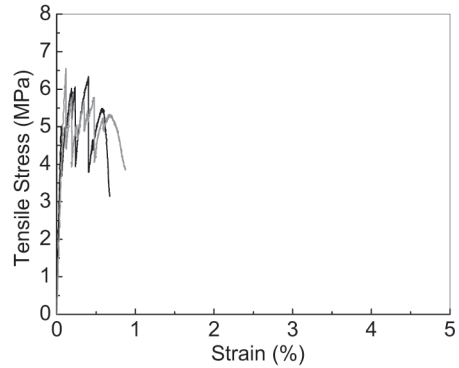


Figure 4. Stress vs. strain curves of Mix 1

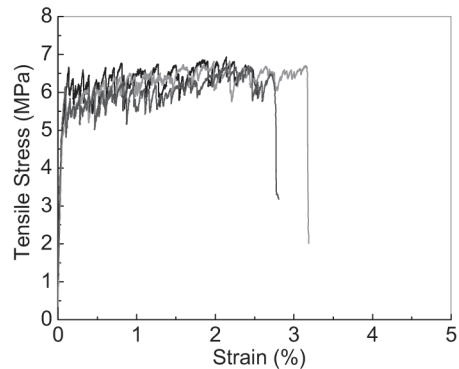


Figure 5. Stress vs. strain curves of Mix 2

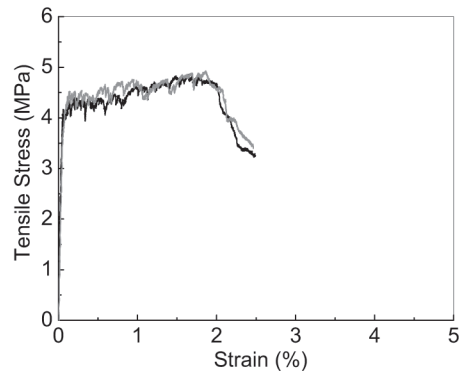


Figure 6. Stress vs. strain curves of Mix 3

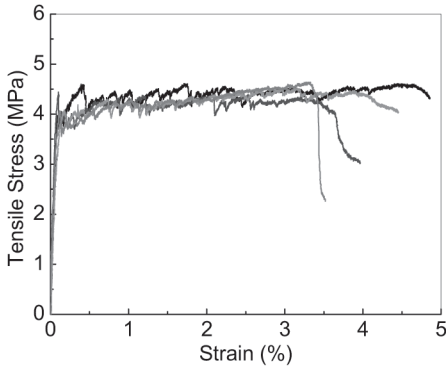


Figure 7. Stress vs. strain curves of Mix 4

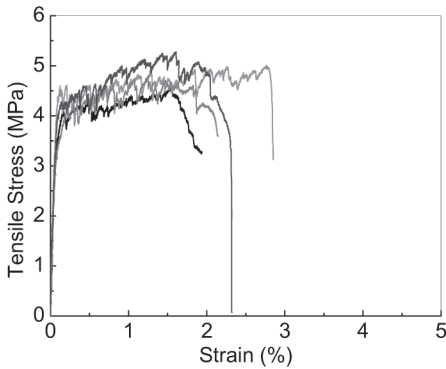


Figure 8. Stress vs. strain curves of Mix 5

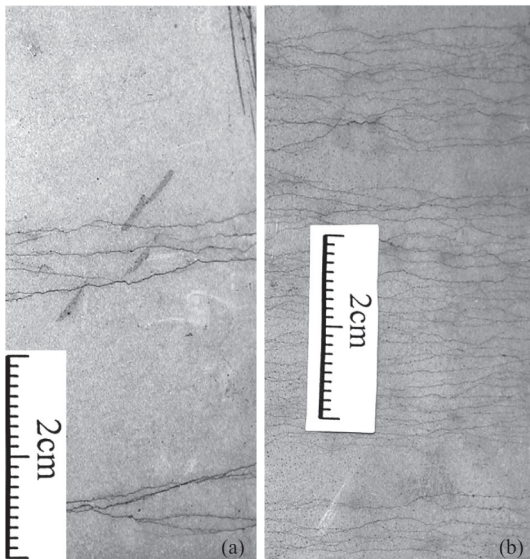


Figure 9. Multiple cracking pattern of Mix 1 (a) and Mix 2 (b)

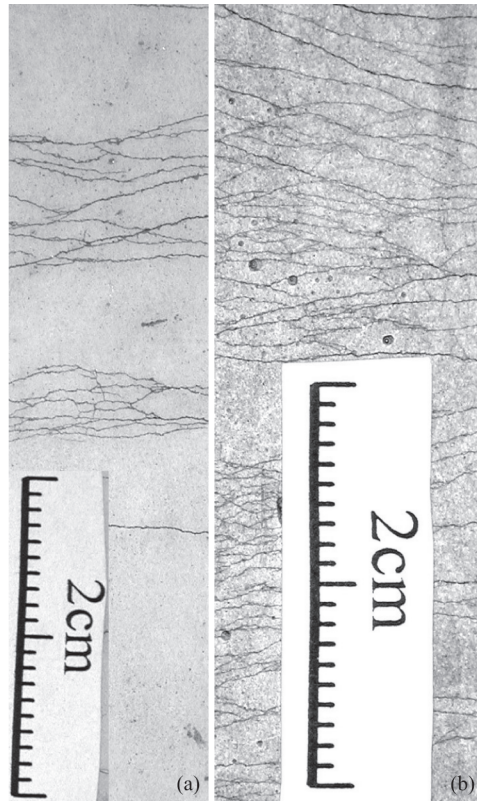


Figure 10. Multiple cracking pattern of Mix 3 (a) and Mix 4 (b)

Attempt was made to characterize the size distribution of large flaws in Mix 1 and 3, by examining the cracked and uncracked sections sliced from the coupon specimen after uniaxial testing under 200× optical microscope. It was found that large flaws are mostly entrapped air voids. The measured size distribution is plotted in Figure 11, where each dot represents one void on the section. With few exemptions, two general observations can be made: 1) the largest void at cracked sections are larger than that on uncracked sections; 2) the number of large voids (>1.0 mm) on cracked sections is higher than that on uncracked sections. This suggests that the large voids play significant role in cracking initiation, provided that the density of capillary pores and small air voids remain almost the same across the specimen. The largest voids on the cracked sections of Mix 1 range from 2.5 mm to 5 mm with an average of 3.4 mm, while the largest voids on the cracked sections of Mix 3 range from 1.7 mm to 4.2 mm with an average of 2.8 mm. Although the void size of Mix 3 is smaller than that of Mix 1, the matrix cracking strength of Mix 1 is generally higher than that of Mix 3. This may be attributed to the difference of matrix fracture toughness between

these two mixes, as matrix K_{IC} is measured as 0.67 and 0.61 $\text{MPa}\cdot\text{m}^{1/2}$ for Mix 1 and Mix 3 respectively.

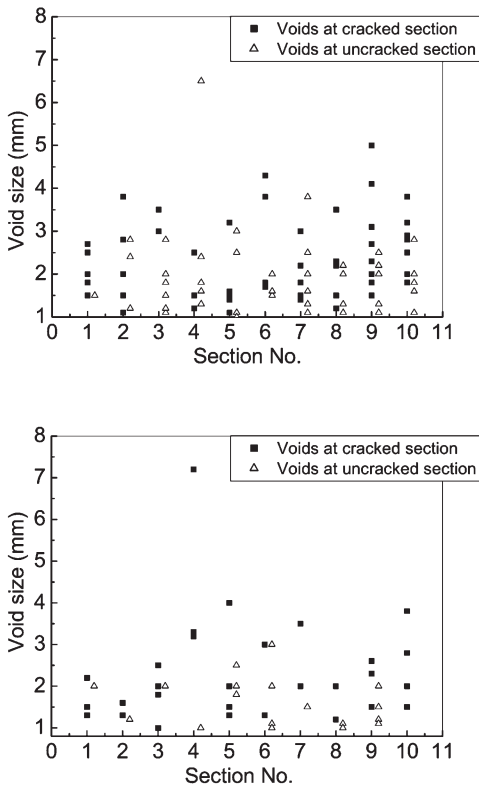


Figure 11. Void size distribution at crack and uncracked sections of Mix 1 (top) and Mix 3 (bottom)

Significant improvement in strain capacity was observed in Mix 2 and 4 with the addition of relatively large artificial flaws, and in both cases multiple cracking exhibits nearly saturated pattern (Fig. 9b & Fig. 10b). For Mix 2, the ultimate strain increases from 0.38% of Mix 1 to 2.48%, and the average crack spacing drops from 16.2 mm to 2.4 mm. For Mix 4, the average strain capacity improves more than 100% from that of Mix 3, accompanied by decrease of average crack spacing from 4.8 mm to 2.2 mm. The presence of the artificial flaws shows negligible influence on the ultimate strength, while it slightly reduces the first cracking strength. In steady state cracking, the matrix cracking strength is lower bounded by the steady state stress. Since the size of the introduced artificial flaws is close to the largest voids in the matrix, it is not surprising that the presence of additional flaws has little effect on the matrix cracking stress.

In saturated multiple cracking, the crack spacing should ideally fall between x_d and $2x_d$, where x_d is the minimum distance which matrix stress needs to reach cracking level by transferring stress from the fiber through interface friction from the adjacent crack. Following Wu & Li (1995), x_d in randomly distributed short fiber composite can be estimated by:

$$x_d = \frac{1}{2} \left(L_f - \sqrt{L_f^2 - \frac{(1-V_f)\sigma_{mu}L_f d_f(4+f^2)}{V_f\tau_0(1+e^{f/2})}} \right) \quad (4)$$

where L_f and d_f are fiber length and diameter respectively; V_f is the fiber volume fraction; τ_0 is the interface frictional stress; f is the fiber snubbing coefficient; and σ_{mu} is the matrix cracking strength. τ_0 is measured as 3.5 and 2.7 MPa for Mix 2 and 4 respectively. Assuming $f=0.7$, which is typical for PVA-ECC system, and using ultimate strength instead of matrix cracking strength for σ_{mu} , the calculated x_d is 1.09 mm and 1.02 mm for Mix 2 and 4 respectively. The measured crack spacing in Mix 2 and 4 slightly exceeds the theoretical upper limit $2x_d$, but is reasonably close.

The importance of controlling the size of the artificial flaws is demonstrated by the results of Mix 5. The Norlite particles used in Mix 5 (1 mm) is much smaller than many voids found at the section; in contrast, the size of the artificial flaws introduced in Mix 2 and 4 are comparable to the size of the largest voids. As a result, no significant improvement in multiple cracking behavior and strain capacity is observed in Mix 5 compared to the control mix, even if the number of the artificial flaws in Mix 5 is much higher than that in Mix 4.

5 CONCLUSION

The viability to achieve saturated multiple cracking in ECC through tailoring of pre-existing flaw size distribution in matrix is demonstrated in this study. A practical approach to modify the flaw size distribution, i.e. by introducing artificial flaws with prescribed sizes, is proposed and verified in PVA-ECC system. The experimental results confirm that near saturated multiple cracking can be achieved in PVA-ECC with relatively high toughness matrix by adding sufficient number of large size artificial flaws, providing that the steady state criteria is satisfied in the composite system. Particles with weak bond to cementitious matrix or low strength, e.g. plastic beads and lightweight aggregates, can be used as a source of artificial flaws. It is also

found that controlling the size of the artificial flaws is essential to the effectiveness of this approach.

REFERENCES

- Kanda, T. & Li, V. C. 1998. Multiple cracking sequence and saturation in fiber reinforced cementitious composites. *JCI Concrete Research and Technology* 9(2):19- 33.
- Leung, C. K. Y. 1996. Design criteria for pseudoductile fiber-reinforced composites. *J. Engineering Mechanics* 122(1):10-18.
- Li, V.C. 1992. Post-crack scaling relations for fiber-reinforced cementitious composites. *ASCE J. of Materials in Civil Engineering* 4(1):41-57.
- Li, V.C. 1998. Engineered cementitious composites - tailored composites through micromechanical modeling. In N. Banthia, A. Bentur, A. & A. Mufti (eds.) *Fiber Reinforced Concrete: Present and the Future*: 64-97. Montreal:Canadian Society for Civil Engineering.
- Li, V. C., and Leung, C.K.Y., "Steady State and Multiple Cracking of Short Random Fiber Composites", *ASCE J. of Engineering Mechanics*, Vol. 188, No. 11, pp. 2246-2264
- Li, V.C., Mishra, D.K. & Wu, H.C. 1995. Matrix design for pseudo strain-hardening fiber reinforced cementitious composites. *RILEM J. Materials and Structures* 28(183):586-595.
- Li, V. C., Wu, C., Wang, S., Ogawa, A. & Saito, T. 2002. Interface tailoring for strain-hardening PVA-ECC. *ACI Materials Journal* 99(5): 463-472.
- Lin, Z., Kanda, T. & Li, V.C. 1999. On interface property characterization and performance of fiber reinforced cementitious composites. *J. Concrete Science and Engineering, RILEM* 1:173.
- Marshall, D. B., Cox, B. N. & Evans, A. G. 1985. The mechanics of matrix cracking in brittle-matrix fiber composites. *Acta Metallurgica* 33(11):2013-2021.
- Naaman, A. E., & Reinhardt, H. W. 1996. Characterization of high performance fiber reinforced cement composites. In A. E. Naaman & H. W. Reinhardt (eds.), *Proceedings of 2nd International Workshop on HPRCC, RILEM, No. 31*:1-24. London:E&FN Spon.
- Sujivorakul, C. 2002. Development of high performance fiber reinforced cement composites using twisted polygonal steel fibers. Ph.D. Thesis, University of Michigan.
- Wang, S. & Li, V. C. in prep. Development of green engineered cementitious composites with high volume of fly ash.
- Wu, H.C. & Li, V.C. 1995. Stochastic process of multiple cracking in discontinuous random fiber reinforced brittle matrix composites. *Int'l of J. of Damage Mechanics* 4(1): 83-102, 1995.